Bulgarian Chemical Communications, Volume 49, Special Edition K2, (pp. 38 – 43) 2017

Influence of hydraulic flow and clay hydration on pore pressure and collapse pressure of swelling shale

H.B. Liu*, F. Zhang, Y.F. Meng, G. Li, G.D. Zhang

Laboratory of Oil and Gas Reservoir Geology and Exploration, Southwest Petroleum University, Xindu, Chengdu, 610500 China

Received July 12, 2017; Accepted December 20, 2017

A modified model for wellbore instability of shale formations is developed by considering the coupled flows of water and ions, crystal hydration and osmotic hydration of clay minerals. Based on the thermodynamic theory, we proposed new models to describe the hydraulic flow of water solutions and chemical diffusion of ions, taking into account the permeability and porosity of formation. Simultaneously, we deduced a new expression for the total stress controlling the clay crystal swelling and osmotic swelling with the energy balance between adjacent clay crystals and the diffuse double layer theory. Theoretical simulation indicates that the effects of clay hydration swelling are related to formation water, drilling fluid and ion salinity, as well as the spacing between adjacent clay crystals, and clay crystal swelling stress is far higher than the osmotic swelling stress between clay particles when the spacing is shorter than 4 nm. Ultimately, based on the modified effective stress laws, considering the mineral distribution in shale formation, pore size and clay hydration, the borehole stability model of physico-chemical coupling effects in shale was developed.

Key words: swelling shale; coupled flow; clay platelet hydration; osmotic hydration; modified effective stress, pore pressure, equivalent density of collapse pressure.y

INTRODUCTION

Over the past few decades, many researchers have extensively studied the physical and chemical coupling wellbore instability, and several methods have been proposed to analyze wellbore instability mechanics. Monte Carlo molecular modeling simulations were performed to investigate the swelling and shrinking behavior of hydrated Wyoming-type montmorillonites including different counterions [1]. Shi [2] studied the intercalating behavior of positively charged counterions in montmorillonites with Si^{4+}/Al^{3+} substitution in their first internal layer. The driving forces for the hydration of montmorillonites saturated with alkaline-earth cations were investigated by Fabrice [3]. The welling pressure of compact bentonite was estimated by Tom [4] using Gouy-Chapman diffuse layer theory. The wellbore stability of coal formation was studied by Zhao with discrete elements [5]. The wellbore stability in fractured rock formation with considering mud infiltration was studied by Chen [6]. Huang [7] believed that the pore pressure change and swelling pressure development are two main relevant factors in shale wellbore instability issue. Tao [8] believed that the *in-situ* stress state and rock strength were key parameters in evaluating the wellbore instability and studied the poro-thermoelastic effects on wellbore stability. Ghassemi [9] believed mud filtrate invasion due to thermal and chemical effects to be several times larger than hydraulic flow. Tao and Ghassemi [10] studied the poro-thermoelastic effects on *in situ* stresses and rock strength, and found that neglecting heating and cooling effects will underestimate/ overestimate wellbore instability. AL-Bazali [11] evaluated the interaction between drilling fluid and shale and its effect on pore pressure and alterations of mechanical properties around the wellbore. Gelet [12] investigated the influence of diffusion and mass transfer on the pore pressure distribution in dual porous media: porous blocks and fissure network. Wang [13] developed a fluid-solid chemistry model considering fluid flow and ion transmission. The results showed that the pore pressure and stress are lower without consideration of the diffusion potential, and the linear model overestimates the pore pressure and stress around the wellbore. Hang [14] established a chemo-mechanical coupling model of borehole stability in hard brittle shale considering structure characteristics and targeted hydration. Zeynali Roshan [15] developed a coupled chemo-poroplastic model to investigate the change in ion transfer and its effect on pore pressure and effective stresses in chemically active fractured media. Liang [16] studied the wellbore stability of fracture formation considering weakness planes and porous flow. Zhang [17] improved the evaluating model for borehole stability considering bedding planes and rock anisotropy.

*To whom all correspondence should be sent:
E-mail: sunxiaoyu520634@163.com

In this paper, we try to develop a new model for describing the controlling forces between adjacent clay crystals, and the force equation for osmotic hydration swelling with the diffuse double layer theory. Simultaneously, the coupled flow of water and ions induced by gradients in hydraulic pressure and chemical potential is described with the irreversible thermodynamic theory. Finally, the effective stresses and wellbore instability are investigated with the modified effective stress theory.

THEORIES AND MODELS

The coupled flows of water and ions in shale formation can be conveniently described with a nonequilibrium or irreversible thermodynamic theory, and the relationship between flux J_i and driving forces X_j [18-20] can be expressed as follows:

$$J_i = \sum_j L_{ij} X_j \tag{1}$$

The mass flux of the total solution J_V can be expressed as:

$$J_V = -L_{11}\nabla p - RT\sum_{i=1}^{n} L_{1,i+1}\nabla C_i \tag{2}$$

The ion i molar flux J_i can be written as:

$$J_i = -L_{i+1,1}\nabla p - RTL_{i+1,2}\nabla C_i \tag{3}$$

With the continuity equation for the solute and the solvent:

$$\frac{\partial C_i}{\partial t} + \nabla J_i = 0 \tag{4}$$

$$\frac{\partial \rho}{\partial t} + \nabla(\rho J_V) = 0 \tag{5}$$

And the relationship between the density and the pressure:

$$\rho = \rho_0 \exp\left[c_t\left(p - p_0\right)\right] \tag{6}$$

Substituting Eq. 3 into Eq. 4, the equation is obtained for the transport of ion i:

$$\frac{\partial C_i}{\partial t} = L_{i+1,1}\nabla^2 p + RTL_{i+1,2}\nabla^2 C_i \tag{7}$$

Substituting Eqs. 2 and 6 into Eq. 5, the equation is obtained for the transport of hydraulic pressure transmission:

$$\frac{\partial p}{\partial t} = \left(L_{11}\nabla p + RT\sum_{i=1}^{n} L_{1,i+1}\nabla C_i\right)\nabla p + \frac{1}{c_t}\nabla\left(L_{11}\nabla p + RT\sum_{i=1}^{n} L_{1,i+1}\nabla C_i\right) \tag{8}$$

Assuming $(\nabla p)^2 << 1$, $\nabla p \nabla C_i << 1$, $L_{11} = k/\mu$, $RTL_{i+1,2} = D_i$, and in Eq. 7 the coefficient $L_{i+1,1}$ that multiplies the derivative of pressure is proven to be about three orders of magnitude smaller than the other coefficients. Therefore, Eqs. 7 and 8 can be simplified to:

$$\frac{\partial C_i}{\partial t} = D_i\nabla^2 C_i \tag{9}$$

$$\frac{\partial p}{\partial t} = \frac{1}{c_t}\frac{k}{\mu}\nabla^2 p + \frac{1}{c_t}RT\sum_{i=1}^{n} L_{1,i+1}\nabla^2 C_i \tag{10}$$

where, p is the hydraulic pressure, C_i is the ion i concentration, k is the permeability, μ is the fluid viscosity, ρ_0 is the fluid density, R is the universal gas constant, T is temperature in Kelvin, $L_{i,j}$ are the coefficients, c_t is the fluid compressibility, D_i is the ion i diffusivity M_i is the molar mass of ion i, ϕ_0 is the porosity, p_0 is the original pore pressure.

Norrish [21], Parker [22] and Laird [23] have developed a model for describing the clay crystal swelling with the potential energy balance. Here, we want to deduce a new model to describe the forces controlling the clay crystal swelling.

The potential energies of repulsion G_{rp}, attraction G_{at}, resistance G_{rs} between two adjacent clay crystals are [23]:

$$G_{rp} = G_{at} + G_{rs} \tag{11}$$

The potential energy of attraction can be expressed as:

$$G_{at} = \frac{f_i\sigma e}{2\beta_I\left(D + r_s\right)} + \frac{H}{12\pi}\left(\frac{1}{(2D)^2} + \frac{1}{(2D+2Th)^2} + \frac{2}{(2D+Th)^2}\right) \tag{12}$$

And the interlayer diabattivity β_I is defined as:

$$\beta_I = 4\pi\varepsilon_0\left[\left(1+\tanh\left(\frac{2D-C1}{C2}\right)\right)\left(\frac{\varepsilon_B - \varepsilon_C}{2}\right) + \varepsilon_C\right] \tag{13}$$

The potential energy of repulsion can also be written as:

$$G_{rp} = \left(\frac{\sigma z_i e}{2r_i} + \frac{\sigma e}{2r_s}\right)\left(\frac{1}{\beta_I} - \frac{1}{\beta_B}\right) + \frac{L_B}{(2D)^{12}} \tag{14}$$

where, e is the unit charge on a proton; f_i is the valence of the interlayer cations; r_s is the effective anionic radius of the negative charge sites; σ is the surface charge density; H is the Hamaker constant; L_B is a constant; Th is the thickness of the crystalline plate; D is one half of the layer separation; β_I is the interlayer diabattivity related to layer separation $2D$; ε_0 is the permittivity of vacuum, and $C1$, $C2$, ε_B and ε_C are empirical constants.

Based on Eq. (12), a model for attractive forces between adjacent crystals can be obtained deriving the potential models with respect to the variable D:

$$p_{ats} = \frac{f_i\sigma e}{2\left[\beta_I\left(D + r_s\right)\right]}\left[\beta_I'\left(D + r_s\right) + \beta_I\right] + \frac{H}{3\pi}\left[\frac{1}{8D^3} + \frac{1}{8\left(D+Th\right)^3} - \frac{2}{(2D+Th)^3}\right] \tag{15}$$

and β_I' is as follows:

$$\beta_I^{'} = 4\pi\varepsilon_0\left(\varepsilon_B - \varepsilon_C\right)\frac{1-\tanh\left(\frac{2D-C1}{C2}\right)^2}{C2} \tag{16}$$

With Eq. (14), a model for describing the repulsive forces can be derived:

$$p_{rps} = \left(\frac{\sigma z_i e}{2r_i} + \frac{\sigma e}{2r_s}\right)\frac{1}{\beta_I^{2}}\beta_I^{'} + \frac{24L_B}{(2D)^{13}} \tag{17}$$

So, with Eqs. 14 17, assuming that the repulsive force is positive, and the attractive forces are negative, a model for the clay crystal swelling force can be expressed as:

$$\begin{aligned} p_{totals} &= \left(\frac{\sigma z_i e}{2r_i} + \frac{\sigma e}{2r_s}\right)\frac{1}{\beta_I}\beta_I^{'} + \frac{24L_B}{(2D)^{13}} \\ &- \frac{f_i \sigma e}{2\left[\beta_I\left(D+r_s\right)\right]}\left[\beta_I^{'}\left(D+r_s\right)+\beta_I\right] \\ &- \frac{H}{3\pi}\left[\frac{1}{8D^3} + \frac{1}{8(D+T)^3} - \frac{2}{(2D+T)^3}\right] \end{aligned} \tag{18}$$

Besides the model for clay crystal swelling, we adopt the diffuse double layer theory to model the osmotic swelling force between clay particles [24]. The repulsive force controlling osmotic swelling can be written as:

$$p_{rpo} = 64nkT\kappa^2 \exp\left[-2\left(\frac{2ne^2z^2}{\varepsilon_r\varepsilon_0 kT}\right)^{1/2} D\right] \tag{19}$$

$$\kappa = \frac{\exp(Z/2)-1}{\exp(Z/2)+1} \tag{20}$$

$$Z = ze\psi_0 / kT \tag{21}$$

$$\psi_0 = (2kT/ze)\sinh^{-1}\left(\sigma_{su}/\left(8n\varepsilon_r\varepsilon_0 kT\right)^{1/2}\right) \tag{22}$$

$$\sigma_{su} = \left(e\cdot CEC\cdot Na\right)/S\times 10^{-5} \tag{23}$$

where, n is the bulk solution electrolyte concentration, k is the Boltzmann constant, T is the temperature in Kelvin, z is the valence of the compensating cations, e is the proton charge, ψ_0 is the surface potential, ε_r is the relative permittivity of the medium, ε_0 is the permittivity of vacuum, σ_{su} is the surface charge density, CEC is the cation exchange capacity, S is the specific surface area, and Na is the Avogadro constant.

Assuming that the thickness of the clay particle is T and the spacing of adjacent clay particles is $2D$, the attractive force can be obtained by:

$$p_{ato} = \frac{H}{3\pi}\left(\frac{1}{(2D)^3} + \frac{1}{(2D+2T)^3} - \frac{2}{(2D+T)^3}\right) \tag{24}$$

where, H is the Hamaker constant.

The osmotic swelling force can be expressed as:

$$\begin{aligned} p_{totalo} &= p_{rpo} - p_{ato} = 64nKT\gamma^2 \mathrm{e}^{-2\kappa D} \\ &- \frac{H}{3\pi}\left[\frac{1}{(2D)^3} + \frac{1}{(2D+2T)^3} - \frac{2}{(2D+T)^3}\right] \end{aligned} \tag{25}$$

The clay-water system in shale formation is simplified as a series of single clay platelets connected to a pore [25-29], and presented in Fig. 1.

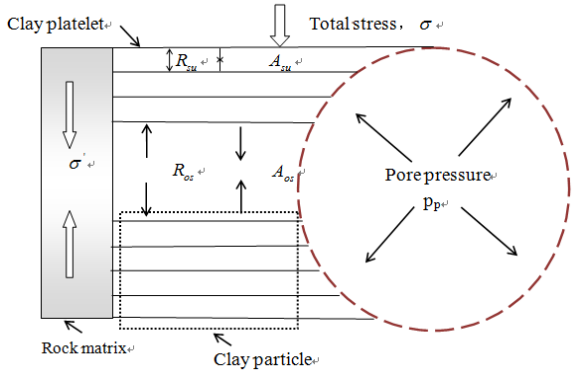

Fig. 1. Simplified structure of the clay-water system in shale formation

According to Fig. 1, the effective stress acting on the rock matrix can be written as:

$$\begin{aligned} \sigma_{i,j}^{eff} &= \sigma_{totali,j} - \alpha p_p^{all}\delta_{i,j} \\ &= \sigma_{totali,j} - \alpha(p_p + p_{swell})\delta_{i,j} \end{aligned} \tag{26}$$

where, $\sigma^{eff}{}_{i,j}$ is the effective stress; $\sigma_{total_{i,j}}$ is the total stress; α is Biot's constant; p_p is pore pressure; p_{swell} is the clay swelling stress; p_{totals} is the clay crystal swelling stress; and p_{totalo} is the osmotic swelling stress.

The stresses around the wellbore in a deviated well can be obtained with the Cartesian coordinate conversion, and expressed as:

$$\begin{bmatrix} \sigma_x & \tau_{xy} & \tau_{xz} \\ \tau_{xy} & \sigma_y & \tau_{yz} \\ \tau_{xz} & \tau_{yz} & \sigma_z \end{bmatrix} = T\begin{bmatrix} \sigma_H & 0 & 0 \\ 0 & \sigma_h & 0 \\ 0 & 0 & \sigma_v \end{bmatrix}T^T \tag{27}$$

and

$$T = \begin{bmatrix} \cos\beta\cos\alpha & \cos\beta\sin\alpha & -\sin\alpha \\ -\sin\alpha & \cos\alpha & 0 \\ \sin\beta\cos\alpha & \sin\beta\sin\alpha & -\cos\beta \end{bmatrix} \tag{28}$$

where, α is the azimuth angle; β is the inclination angle.

So, the stresses around the wellbore can be written as:

$$\begin{aligned} \sigma_x &= \cos^2\gamma\left(\sigma_H\cos^2\beta + \sigma_h\sin^2\beta\right) + \sigma_V\sin^2\beta \\ \sigma_y &= \sigma_H\sin^2\beta + \sigma_h\cos^2\beta \\ \sigma_z &= \sin^2\gamma\left(\sigma_H\cos^2\beta + \sigma_h\sin^2\beta\right) + \sigma_V\cos^2\gamma \\ \tau_{xy} &= \cos\gamma\sin\beta\cos\beta\left(\sigma_h - \sigma_H\right) \\ \tau_{xz} &= \cos\gamma\sin\gamma\left(\sigma_H\cos^2\beta + \sigma_h\sin^2\beta - \sigma_V\right) \\ \tau_{yz} &= \sin\gamma\cos\beta\sin\beta\left(\sigma_h - \sigma_H\right) \end{aligned} \tag{29}$$

Based on the Drunker-prager criterion, the minimum drilling fluid density maintaining wellbore stability can be obtained as follows:

$$\rho_m = \frac{-B-\sqrt{B^2-4b}}{2H}\times 100 \qquad (30)$$

where

$$B = -3\sigma_H + \sigma_h$$

$$b = \frac{1}{6}\left[\left(3\sigma_H-\sigma_h\right)^2+\left(3\sigma_H-\sigma_h-\sigma_v\right)^2+{\sigma_v}^2\right]$$

$$-\left[\frac{\sqrt{3}\sin\varphi}{3\sqrt{3+\sin\varphi^2}}(3\sigma_H-\sigma_h-\sigma_v-3\alpha(p_p+p_{swell}))\right]^2$$

$$-\frac{\sin 2\varphi}{2\sqrt{3+\sin\varphi^2}}(3\sigma_H-\sigma_h-\sigma_v-3\alpha(p_p+p_{swell}))-\frac{3C^2\cos\varphi^2}{3+\sin\varphi^2}$$

where, σ_H and σ_h are the maximum and minimum principal stresses; C is the cohesion; φ is the internal friction angle; and H is the depth.

RESULTS AND DISCUSSION

The input data used to calculate the coupled flow of water and ions are presented in Table 1. The coefficient L describes the chemical effect on the hydraulic flow, and it is negative in Lomba's paper [30]. Applying the experimental data in Table 1, the pore pressure and ion concentration distribution of fluid in the near wellbore zone are calculated, and are shown in Figs. 2 and 3.

Table 1. Input data

Parameters	Value
p_0	30MPa
p_w	45MPa
C_0	2000mol.m^{-3}
C_{df}	1000 mol.m^{-3}
k	3×10^{-19}m^2
c_t	4.35×10^{-4}MPa^{-1}
D	10^{-10}m^{2}s^{-1}
μ	10^{-9}MPa.s
R	8.314J.mol^{-1}K^{-1}
T	300K
L	-4.38×10^{-17}MPa.m.s

As shown in Figs. 2 and 3, when the shale formation is opened, water-based drilling fluid quickly flows into the shale formation under the pressure gradient and the chemical potential gradient, the pore pressure in the wellbore surface increases to the bottom pressure in a short time, and the increasing rate depends on the pressure difference between the original pore pressure and bottom pressure.

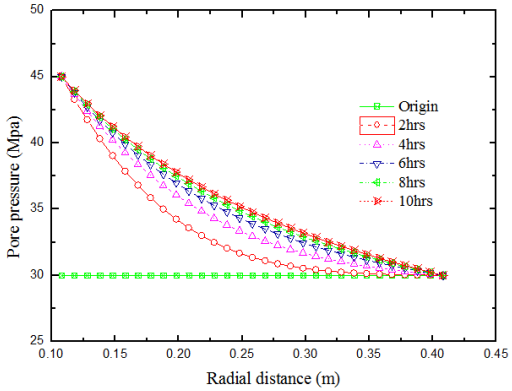

Fig.2. Pore pressure profiles as a function of time

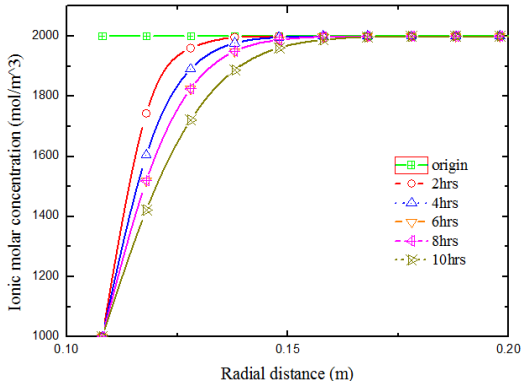

Fig.3. Solute concentration profiles as a function of time

We calculated the clay crystal swelling and osmotic swelling with the basic data in Table 2.

Table 2. Basic input data

Parameters	Value
σ	0.193C.m^{-2}
e	1.602×10^{-19}C
D	7.5×10^{-10}m
H	10^{-20}J
T	9.6×10^{-10}m
r_s	4.7×10^{-10}m
r_i	3.58×10^{-10}m
β_B	8.695×10^{-9}C^{-2}N^{-1}m^{-2}
ε_B	78
ε_C	6
L_B	1.4627×10^{-124}J.m^{10}

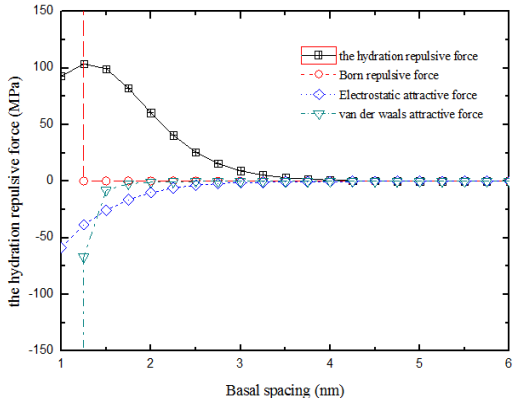

Fig. 4. Relationship between interlayer forces and basal spacing

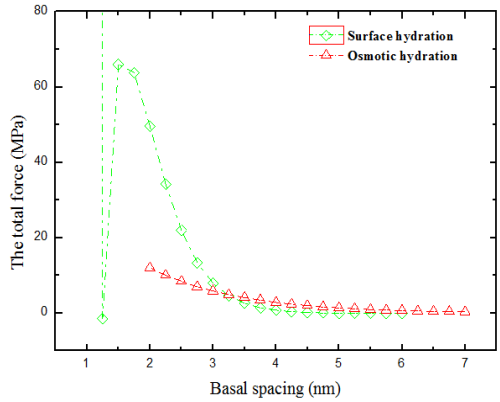

Fig. 5. Comparison of the total forces for surface hydration and osmotic hydration

Fig. 4 compares all forces of interlayer and their relationship with basal spacing. When the basal spacing is very small, born repulsive force and Van der Waals attractive force are super high. Once one layer of water molecules is adsorbed, born repulsive force and Van der Waals attractive force would rapidly decrease. Born repulsive force decreases to 0 and Van der Waals decreases to 0 for a spacing of 2 nm. Relatively, the hydration repulsive forces and the electrostatic attractive force decrease more slowly, the electrostatic attractive force drops to 0 when the basal spacing is about 3 nm, and the hydration repulsive forces drop to 0 for a spacing about 4 nm.

Fig. 5 shows that there are significant differences between surface hydration swelling force and osmotic hydration swelling force. The total force of surface hydration is super high for a basal spacing of 1 nm, and then drops to about 0 for a basal spacing of 1.25 nm.

The pore pressure, effective stresses and collapse force are evaluated with the modified effective stress law.

As shown in Fig. 6, the original formation pressure is 30 MPa, and the coupled flows and the clay swelling cause pore pressure on the wellbore wall to increase to 55.65 MPa.

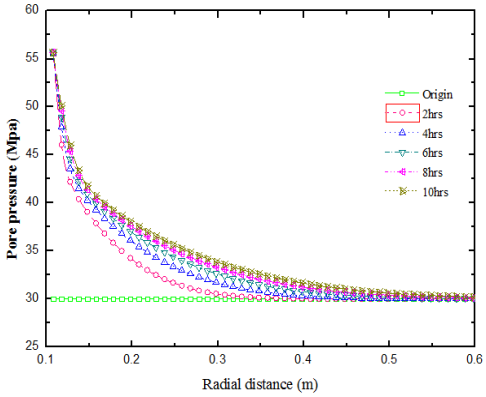

Fig. 6. Pore pressure distributions by considering coupled flows and clay hydration swelling

Fig. 7 shows that the increase in the pore pressure in the near wellbore zone leads to a continuous reduction of the effective radial stress and the effective hoop stress on the rocks.

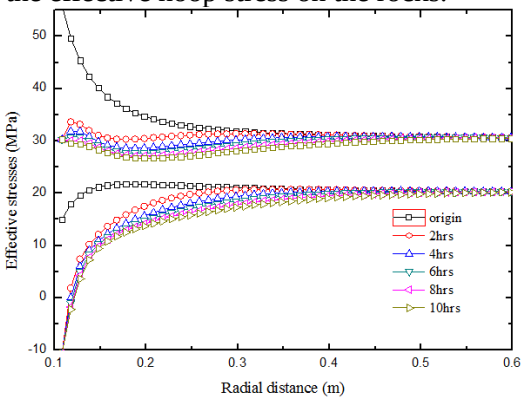

Fig. 7. Effective stresses distribution around wellbore

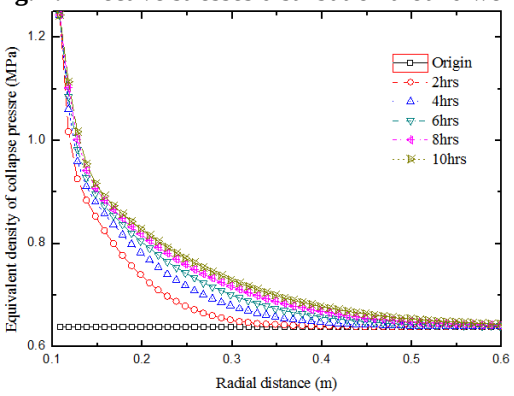

Fig. 8. Distribution of the equivalent density of collapse pressure

Fig. 8 indicates that both the penetration of the drilling fluid into the formation and the clay hydration swelling lead to a sharp increase of the collapse pressure in the near wellbore zone. The increasing amount on the rock surface is approximately 100% for the equivalent density to increase from 0.639 g/cm^3 to 1.244 g/cm^3. This is the reason why the borehole is unstable using conventional water-based drilling fluid but stable in gas drilling.

CONCLUSION

This paper deduces the coupled flow of the water solution and its components on the basis of the irreversible thermodynamic theory. The results indicate that the effect of clay permeable membrane on the pore fluid flow is not significant. Combining with the potential equilibrium equation controlling the clay crystal swelling potential, the equilibrium equation for forces controlling the clay crystal swelling was developed. Ultimately, based on the modified effective stress laws, considering the physical-chemical coupled flow of the pore fluid in the shale formation and the clay hydration swelling effect, as well as the calculation models for the pore pressure, the effective stresses and the equivalent density of collapse pressure in shale formation were developed. The calculation results indicated that the

coupled flow of the drilling fluid in the formation, the clay crystal swelling and the clay osmotic swelling have a significant effect on the borehole stability, and also showed that the effect of the clay crystal swelling is more significant than that of osmotic swelling.

REFERENCES

1. Y. Zheng， A. Zaoui， I. Shahrour, *Applied Clay Science*, **51**(1), 177 (2011).
2. J. Shi，H. Liu，Z. Lou，Y. Zhang，Y. Meng, Q. Zeng, M. Yang, et al., *Computational Materials Scienc*e, **69**, 95 (2013).
3. F. Salles， J.M. Douillard， O. Bildstein， C. Gaudin，B. Prelot, J. Zajac, H. Van Damme, *Journal of colloid and interface scienc*e, **395**, 269 (2013).
4. T. Schanz， M.I. Khan， Y. Al-Badran, Applied Clay Science, **8**3, 383 (2013).
5. H. Zhao，M. Chen，Y. Li，W. Zhang, *International Journal of Rock Mechanics and Mining Sciences*, **5**4, 43 (2012).
6. X. Chen， C.P. Tan， C. Detournay, *Journal of Petroleum Science and Engineerin*g, **38**(3), 145 (2003).
7. H. Huang，J.J. Azar，A. Hale, Numerical simulation and experimental studies of shale interaction with water-base drilling fluid. 1998.
8. Q. Tao，A. Ghassemi, *Geothermics*, **39**(3), 250 (2010).
9. A. Ghassemi，A. Diek, *Journal of Petroleum Science and Engineering*, 2002. **34**(1): p. 123-135.
10. R. Gelet， B. Loret， N. Khalili, *International Journal of Rock Mechanics and Mining Science*s, **50**, 65 (2012).
11. Q. Wang，Y. Zhou，G. Wang，H. Jiang，Y. Liu, *Petroleum Exploration and Development*, **39**(4), 508 (2012).
12. S. He， W. Wang， M. Tang， B. Hu， W. Xue, Journal of Natural Gas Science and Engineering, **21**, 338 (2014).
13. H. Wen， M. Chen， Y. Jin, K. Wang, Y. Xia, G. Dong, Ch. Niu, *Petroleum Exploration and Development*, **41**(6), 817 (2014).
14. M.E. Zeynali, *Journal of Petroleum Science and Engineering*, **82**, 120 (2012).
15. H. Roshan，M. Fahad, *International Journal of Rock Mechanics and Mining Sciences*, **52**, 82 (2012).
16. E.V. Oort，A.H. Hale，F.K. Mody，S. Roy, *SPE Drilling & Completion*, **11**(03), 137 (1996).
17. R.F.T. Lomba， M.E. Chenevert， M.M. Sharma, Chenevert, M.M. Sharma, *Journal of Petroleum Science and Engineering*, **25**(1–2), 25 (2000).
18. G. Chen，R.T. Ewy，M. Yu, J*ournal of Petroleum Science and Engineering*, **72**(1), 158 (2010).
19. K. Norrish, *Discuss. Faraday Soc*., **18**, 120 (1954).
20. J.C. Parker, *Clays Clay Miner.*, **28**(2), 135 (1980).
21. D. A. Laird, *Clays Clay Miner.*, **44**(4), 553 (1996).
22. N. Alcantar，J. Israelachvili，J. Boles, *Geochimica et Cosmochimica Acta*, **67**(7), 1289 (2003).
23. S.L. Barbour, D.G Fredlund, *Canadian Geotechnical Journa*l, **26**(4), 551 (1989).
24. P.K. Chatterji, N.R. Morgenstern, K.B. Hoddinott，R.O. Lamb, In *Physico-chemical aspects of soils and related materials*, ASTM International, 1095, 118 1990.
25. L. Ge, P. Hu, X.H. Xie, Z. Hu, Q. Zeng, J.B. Liao, *Oxid Commun*, **39**(1), 317 (2016).
26. L. Ge, Z. Hu, P. Chen, L. Shi, Q.Yang, J.B. Liao, *Mathematical Problems in Eng.*, Volume 2014, 1 (2014).
27. L. Ge, Z.Y. Wang, K. Deng, Q. Zeng, X. Wang, X.S. Chen, J.B. Liao, *Journal of the Balkan Tribological Association*, **21**(4), 897 (2015).
28. L. Ge, G.H. Wei, Q. Wang, Z. Hu, J.L.Li, *IEEE Sensors Journa*, **17**(18), 5831 (2017).
29. L. Ge, Q. Zeng, Z.Y. Wang, X.H. Xie, J.B. Liao, J.L. Li, *Oxid Commun*, **39**(1), 240 (2016).
30. R.F.T. Lomba， M.E. Chenevert， M.M. Sharma, *Journal of Petroleum Science and Engineering*, 25(1-2), (2000).